scientific reports

Check for updates

OPEN

EphA2 monoclonal antibody attenuates hyperoxia-induced acute lung injury by preserving the alveolar–endothelial barrier

Kyung Soo Chung[1], Ju Hye Shin[1], Su Hwan Lee[1], Ah Young Leem[1], Moo Suk Park[1], Jong Seok Moon[2,3]✉ & Young Sam Kim[1,3]✉

Supplemental oxygen is essential for acute respiratory distress syndrome (ARDS); however, prolonged exposure to high-inspired oxygen fractions can cause hyperoxia-induced acute lung injury (HALI). Hyperoxia disrupts the alveolar–endothelial barrier through excess reactive oxygen species and inflammation, leading to edema, impaired gas exchange, and increased mortality. EphA2/ephrinA1 signaling regulates cytoskeletal dynamics and intercellular adhesion; however, its role in HALI remains unclear. We hypothesized that pharmacological EphA2 blockade would protect the alveolar–endothelial barrier. Male C57BL/6 J mice were exposed to > 95% O_2 for up to 72 h to establish HALI. Temporal changes in EphA2/ephrinA1 signaling, barrier proteins, and cytokines were assessed at 0, 24, 48, and 72 h. To evaluate therapeutic potential, mice exposed to 72 h hyperoxia received intravenous phosphate-buffered saline (PBS) or anti-EphA2 monoclonal antibody (mAb; 8 µg pretreatment). Lung injury was evaluated through histology, bronchoalveolar lavage (BAL) protein and cytokine levels, and the expression of junctional, apoptotic, and oxidative stress markers using western blotting and immunostaining. Survival was analyzed using Kaplan–Meier. Hyperoxia increased phosphorylated EphA2, disrupted VE-cadherin, ZO-2, and claudin-5, and elevated BAL protein and cytokine levels. EphA2 mAb pretreatment reduced histological injury, preserved junctional proteins, attenuated cytokine responses, enhanced Akt phosphorylation, decreased Bcl-2 levels, and reduced oxidative stress. Survival improved after 72 h of severe hyperoxia ($p = 0.045$). EphA2/ephrinA1 activation contributed to HALI. EphA2 mAb pretreatment mitigated lung injury and preserved barrier integrity, supporting EphA2 blockade as a potential barrier-protective strategy under severe hyperoxic stress.

Keywords EphA2, Ephrina1, Hyperoxia-induced lung injury

Acute respiratory distress syndrome (ARDS) and other causes of acute respiratory failure profoundly impair pulmonary gas exchange and often require invasive mechanical ventilation with high-inspired oxygen fractions. In this context, supplemental oxygen is prescribed as a life-saving intervention. However, the potential for oxygen toxicity has been recognized for decades. Clinical and experimental data indicate that exposure to supraphysiological oxygen tension can trigger hyperoxia-induced acute lung injury (HALI), which is characterized by oxidative stress, alveolar–capillary barrier disruption, and progressive respiratory failure[1–4].

Importantly, hyperoxia is not necessarily the primary driver of lung injury in typical ARDS and ventilator-induced lung injury (VILI), where mechanical forces, biotrauma, and heterogeneous alveolar collapse contribute substantially to VILI. However, sustained high oxygen exposure can be a major contributor to lung injury in contexts (e.g., patients managed with hyperoxic strategies for neurologic indications, post-cardiac arrest care, or during aeromedical evacuation when high FiO_2 is maintained). Accordingly, the HALI model in this study is intended as a mechanism-focused platform to interrogate oxygen-toxicity-driven barrier disruption rather than as a complete surrogate for ARDS.

[1]Division of Pulmonary and Critical Care Medicine, Department of Internal Medicine, Severance Hospital, Yonsei University Health System, 50 Yonsei-ro, Seodaemun-gu, Seoul 03722, Republic of Korea. [2]Department of Integrated Biomedical Science, Soonchunhyang Institute of Medi-Bio Science (SIMS), Soonchunhyang University, 31 Suncheonhyang 6-gil, Dongnam-gu, Cheonan 31151, Korea. [3]These authors contributed equally: Jong Seok Moon and Young Sam Kim. ✉email: jongseok81@sch.ac.kr; ysamkim@yuhs.ac

Although the optimal oxygenation targets for critically ill adults remain controversial, recent randomized trials and meta-analyses comparing conservative and liberal oxygen strategies have underscored that both hypoxemia and sustained hyperoxia may be harmful. Large trials on patients in mechanically ventilated intensive care unit (ICU), including HOT-ICU and ICU-ROX, together with contemporary systematic reviews, have generally failed to show a survival benefit of liberal oxygen therapy and highlighted the potential associations between higher oxygen exposure and adverse outcomes[5–9]. These findings reinforce that oxygen should be regarded as a drug with a narrow therapeutic window, and better understanding of HALI pathobiology is required to inform safer oxygen use at the bedside.

Experimental models have provided important mechanistic insights into HALI. Prolonged exposure to highly inspired oxygen fractions overwhelms endogenous antioxidant defenses, leading to excess reactive oxygen species (ROS) generation, mitochondrial dysfunction, and cell death in the pulmonary epithelium and endothelium.[1,2,4] Hyperoxia promotes pulmonary edema, hyaline membrane formation, and microvascular thrombosis, recapitulating several histological features of human ARDS. Recent studies have implicated ferroptosis, autophagy dysregulation in type II alveolar epithelial cells, and endothelial proteomic remodeling as additional contributors to HALI[10–12]. Despite these advances, effective pharmacological strategies to directly protect the alveolar–endothelial barrier during hyperoxic stress are still lacking.

Erythropoietin-producing hepatoma (Eph) receptors and their ephrin ligands constitute the largest family of receptor tyrosine kinases and have emerged as key regulators of tissue patterning, vascular biology, and inflammation[13,14]. Eph receptors are categorized into the EphA and EphB subclasses based on their sequence homology and binding preferences for glycosylphosphatidylinositol-anchored ephrin-A or transmembrane ephrin-B ligands. EphA2, a prototypical EphA receptor, is widely expressed in epithelial and endothelial cells and can modulate cytoskeletal organization, cell–cell adhesion, and barrier permeability. Experimental lung injury models have shown that EphA2 expression is upregulated in response to viral infection, hypoxia, and bleomycin and that EphA2 activation promotes endothelial permeability and inflammatory cell recruitment[14–16].

In the pulmonary microvasculature, EphA2/ephrinA1 signaling has been linked to the disassembly of tight and adherens junctions, including claudin-5, VE-cadherin, and zonula occludens proteins, as well as the amplification of lung inflammation[14–18]. EphA2 antagonism attenuates lipopolysaccharide-induced acute lung injury and reduces vascular leakage and oxidative stress, suggesting that EphA2 functions as a critical node at the interface of vascular injury and inflammatory signaling[17,18]. Outside the lungs, EphA2 modulates the epithelial barrier integrity in the upper airway and participates in host responses to respiratory pathogens, further emphasizing its relevance in respiratory mucosal biology[19,20]. However, whether EphA2/ephrinA1 signaling contributes specifically to the pathogenesis of hyperoxia-induced lung injury and whether EphA2 blockade can preserve the alveolar–endothelial barrier during severe hyperoxia remains unclear.

Therefore, we investigated the role of EphA2/ephrinA1 signaling in a murine model of HALI and determined whether pharmacological inhibition of EphA2 using a monoclonal antibody could mitigate lung injury. Using prolonged exposure to > 95% oxygen to induce HALI, we first characterized time-dependent changes in EphA2 activation, barrier junction proteins, and inflammatory mediators. We then evaluated whether pretreatment with an anti-EphA2 monoclonal antibody preserved alveolar–endothelial junctional integrity, reduced inflammation and oxidative stress, and improved survival following a lethal hyperoxic insult. By elucidating the contribution of EphA2/ephrinA1 signaling to HALI and testing EphA2 blockade in vivo, this study aimed to provide a mechanistic rationale for targeting EphA2 as a potential therapeutic strategy for oxygen-induced lung injury.

Materials and methods

HALI model and experimental design

HALI was established using a sealed Plexiglas chamber supplied with 100% oxygen at a constant flow rate of 2–4 L/min as previously described. The fraction of inspired oxygen within the chamber was monitored using an oximeter and was maintained at > 95% throughout the exposure period. Control animals were maintained in room air (21% O_2).

We performed three sets of experiments (Additional File 1):

Time-course characterization of HALI and EphA2/ephrinA1 signaling

Mice were exposed to hyperoxia for 0, 24, 48, or 72 h to confirm the reproducibility of the HALI model and assess temporal changes in EphA2/ephrinA1 signaling. At each time point, mice were euthanized by intraperitoneal injection of a lethal dose of Zoletil (30 mg/kg) and xylazine (Rompun, 10 mg/kg). Lung tissue and bronchoalveolar lavage (BAL) fluid were collected for histological assessment, protein leakage, cytokine measurements, and immunoblotting of signaling and junctional proteins.

Evaluation of EphA2 monoclonal antibody treatment at 72 h

For determining the effect of EphA2 blockade on established HALI, 12 mice were randomly allocated to three groups at the level of the individual mouse within each cage to minimize cage effect: (i) normoxia plus phosphate-buffered saline (PBS), (ii) hyperoxia plus PBS, and (iii) hyperoxia plus EphA2 monoclonal antibody (EphA2 mAb). EphA2 mAb (8 μg; R&D Systems, Minneapolis, MN, USA) was administered via tail vein injection as a pretreatment before initiation of hyperoxia. All mice were exposed to hyperoxia for 72 h and euthanized to collect BAL fluid and lung tissue. The dose of 8 μg was selected based on preliminary experiments showing superior protection against BAL protein leakage compared with 4 μg. (Additional File 2).

Survival analysis after hyperoxic insult

Prolonged exposure to > 95% oxygen for more than 72 h is uniformly lethal in this model, with an expected mortality of approximately 60%–80% when the mice are returned to room air. Therefore, we used post-hyperoxic

survival as an index of injury severity and treatment efficacy. Mice were exposed to hyperoxia for 72 h, returned to normoxia (21% O_2), and survival was monitored thereafter. Two groups were compared: (i) hyperoxia plus intravenous PBS and (ii) hyperoxia plus intravenous EphA2 mAb (8 μg). Each group included 14 animals as shown in the figure legends.

BAL and cell analysis

BAL was performed immediately after euthanasia using a tracheal cannula. The lungs were gently lavaged with two sequential 1 mL sterile saline aliquots. The recovered BAL fluid was pooled and centrifuged at 400 × *g* for 10 min at 4 °C. The supernatant was aliquoted and stored at – 80 °C for subsequent protein and cytokine analyses. The cell pellet was resuspended in 100 μL PBS.

Total BAL cell counts were determined using a hemocytometer, according to the manufacturer's instructions. For differential cell counts, 90 μL cell suspension was loaded into cytospin chambers, centrifuged at 600 rpm for 6 min, air-dried, and stained with a three-step Diff-Quik protocol (fixative, solution I, solution II), followed by rinsing in distilled water. Differential counts were performed on the stained cytospin preparations using light microscopy.

BAL protein concentration was measured using a bicinchoninic acid (BCA) protein assay kit (Pierce BCA, Thermo Fisher Scientific, Rockford, IL, USA). After incubation at 37 °C for 30 min, the absorbance was recorded at 562 nm using a microplate spectrophotometer, and protein concentrations were calculated from a standard curve.

Lung histology and injury scoring

After BAL, pulmonary circulation was flushed with saline under low pressure through the right ventricle. The right lung was snap-frozen at – 80 °C for protein extraction. The left lung was inflated via tracheostomy with 10% neutral buffered formalin in PBS at a constant pressure of 25 cm H_2O until the pleural margins became sharp. The inflated lung was then excised, fixed overnight in 10% formalin, processed, embedded in paraffin, and sectioned at 5-μm thickness.

Sections were stained with hematoxylin and eosin (H&E) and examined using light microscopy. Lung injury was semi-quantitatively assessed in a blinded fashion by two independent investigators using the weighted scoring system recommended by the American Thoracic Society for Experimental Acute Lung Injury. Five pathological features (alveolar and interstitial edema, hemorrhage, inflammatory cell infiltration, hyaline membrane formation, and atelectasis) were graded, and composite lung injury scores were calculated.

Cytokine and chemokine measurements in BAL fluid

The concentrations of selected cytokines and chemokines in BAL fluid were quantified using a multiplex Magnetic Luminex® Screening Assay kit, according to the manufacturer's instructions. All standards and samples were run in duplicate and analyzed on a Luminex MAGPIX platform (Bio-Techne, Minneapolis, MN, USA). The panel included interleukin (IL)-1β, IL-6, IL-10, tumor necrosis factor-α (TNF-α), keratinocyte-derived chemokine/CXCL1, and macrophage inflammatory protein-2 (MIP-2/CXCL2).

Protein extraction and western blotting

Frozen lung tissue was homogenized in ice-cold radioimmunoprecipitation assay (RIPA) buffer (50 mM Tris–HCl, pH 7.5; 150 mM NaCl; 1% Triton X-100; 1% sodium deoxycholate; 0.1% sodium dodecyl sulfate; and 2 mM ethylenediaminetetraacetic acid) supplemented with a protease inhibitor cocktail. Homogenates were incubated on ice for 20 min and centrifuged at 14,000 × *g* for 15 min at 4 °C. The supernatant was collected, mixed with 5 × SDS sample buffer, boiled for 5 min, and stored at – 80 °C until use.

Equal amounts of protein were separated on Tris–glycine gradient gels (Q-PAGE™, SMOBIO Technology, Hsinchu City, Taiwan) and transferred to polyvinylidene difluoride membranes (Millipore, Billerica, MA, USA). The membranes were blocked for 1 h at room temperature in Tris-buffered saline containing 0.05% Tween-20 (TBS-T) and 5% nonfat dry milk.

The blots were incubated overnight at 4 °C with primary antibodies against EphA2, ephrinA1, Bcl-2, and ZO-2 (Santa Cruz Biotechnology, Dallas, TX, USA); EphA2 and ephrinA1 (Thermo Fisher Scientific, Rockford, IL, USA); phospho-EphA2, E-cadherin, phospho-Akt, and total Akt (Cell Signaling Technology, Danvers, MA, USA); EphB4, ephrinB2, VE-cadherin, NOX4, Keap1, and vascular endothelial growth factor (VEGF; Abcam, Cambridge, UK); and β-actin (Sigma-Aldrich, St. Louis, MO, USA). After five washes in TBS-T, the membranes were incubated for 1 h at 37 °C with horseradish peroxidase-conjugated secondary antibodies (anti-rabbit, anti-rat, or anti-mouse IgG; 1:2000 dilution; Thermo Fisher Scientific). After additional washes, bands were visualized using enhanced chemiluminescence reagents (Thermo Fisher Scientific) and captured on a photographic film. Only linear adjustments to brightness and contrast were applied uniformly to the entire image. No nonlinear adjustments, selective enhancement, or removal of bands were performed. Densitometric analysis was performed using standard image analysis software, with β-actin serving as a loading control.

Immunohistochemical analysis and immunofluorescence

Formalin-fixed, paraffin-embedded lungs were serially sectioned for immunohistochemical analysis (IHC) and immunofluorescence (IF). For IHC, the sections were stained using an automated immunostainer (DAKO Autostainer Link 48) with primary antibodies against VEGF, VE-cadherin, and claudin-5 (Abcam; 1:50). Detection was performed using an appropriate secondary system and a chromogenic substrate, followed by hematoxylin counterstaining using an H&E stainer (Leica Autostainer XL, CV5030).

For IF, 4 μm sections were deparaffinized, rehydrated, permeabilized in 0.5% Triton X-100 (Sigma-Aldrich), and blocked with CAS-Block™ Histochemical Reagent (Thermo Fisher Scientific). Sections were incubated

with polyclonal rabbit anti–4-hydroxynonenal (4-HNE) antibody (1:100, ab46545, Abcam) and monoclonal mouse anti-E-cadherin antibody (1:100, sc-8426, Santa Cruz Biotechnology). After washing, the sections were incubated with goat anti-rabbit IgG (H + L) Alexa Fluor 488 (1:100, A11008, Thermo Fisher Scientific) and goat anti-mouse IgG (H + L) Texas Red (1:100, ab6787, Abcam) for 2 h at 25 °C. Nuclei were counterstained with Fluoroshield™ mounting medium containing DAPI (Sigma-Aldrich).

Fluorescent images were acquired using a THUNDER Imager Tissue microscope (Leica Microsystems, Wetzlar, Germany). The signal intensity and area of positive staining were quantified using the LAS X software (Leica Microsystems) and ImageJ software (National Institutes of Health, Bethesda, MD, USA). All image analyses were performed under identical settings by two independent observers who were blinded to group allocation.

Statistical analysis

Data are presented as median (interquartile range, IQR) for box-and-whisker plots and as mean ± standard deviation (SD) or mean ± standard error of the mean (SEM) for bar graphs, as specified in the figure legends. Each dot represents one mouse; duplicate technical measurements were averaged per mouse. Group comparisons were performed using two-sided unpaired *t*-tests or one-way analysis of variance (ANOVA) with Bonferroni's multiple-comparison test. Survival curves were generated using the Kaplan–Meier method and compared using log-rank tests. Statistical analyses were conducted using the GraphPad Prism software (version 5.0; GraphPad Software, San Diego, CA, USA). A two-sided p-value < 0.05 was considered statistically significant.

Results

Time-dependent development of hyperoxia-induced lung injury and EphA2/ephrinA1 activation

Prolonged exposure to > 95% oxygen results in progressive structural and inflammatory lung injury. Compared to normoxic controls, mice exposed to hyperoxia for 24, 48, and 72 h exhibited increasingly severe histopathological changes, including alveolar and interstitial edema, inflammatory cell infiltration, and hyaline membrane formation. These changes were reflected by a stepwise increase in composite lung injury scores and BAL protein concentrations, indicating disruption of the alveolar–endothelial barrier (Additional Files 3A, 3C).

Hyperoxia elicits robust inflammatory responses. IL-1β, TNF-α, IL-6, and MIP-2 levels in BAL fluid rose in a time-dependent manner with increasing duration of oxygen exposure (Additional File 3E). Consistent with barrier injury, the expression of tight and adherens junction proteins, including VE-cadherin, VEGF, and ZO-2, progressively reduced in the lung tissue, as demonstrated by immunoblotting and immunostaining (Additional Files 3G, 3H). These changes were most pronounced after 72 h of hyperoxia.

At the signaling level, hyperoxia induces the activation of pro-survival and stress pathways. Phosphorylated Akt and anti-apoptotic protein Bcl-2 levels increased over time in hyperoxic lungs, which is consistent with previous observations that Akt activation is accompanied by early endothelial damage under hyperoxic conditions. In parallel, phosphorylated EphA2 expression was upregulated with prolonged oxygen exposure, whereas changes in EphB4/ephrinB2 expression were less prominent, suggesting preferential involvement of EphA2/ephrinA1 signaling in HALI.

EphA2 monoclonal antibody improves lung injury and survival after hyperoxia

To test whether EphA2 blockade attenuates HALI, the mice were randomized to receive normoxia plus PBS, hyperoxia plus PBS, or hyperoxia plus EphA2 mAb. Representative H&E-stained sections showed that EphA2 mAb treatment reduced alveolar edema, vascular congestion, and hyaline membrane formation compared with hyperoxic PBS treatment (Fig. 1A). Quantitatively, the lung injury scores were significantly lower in the EphA2 mAb group ($p = 0.012$), indicating substantial histological protection (Fig. 1C). BAL protein concentrations were increased under hyperoxia (PBS). When comparing the two hyperoxia groups, EphA2 mAb pretreatment showed a lower BAL protein concentration relative to the PBS group; however, this difference did not reach statistical significance, indicating a trend toward reduced protein leakage. (Fig. 1B).

Next, we evaluated whether the EphA2 blockade translated into improved survival following a severe hyperoxic insult. The mice were exposed to > 95% oxygen for 72 h, returned to room air, and survival was monitored. In the absence of treatment, hyperoxia is associated with high mortality rates. Pretreatment with EphA2 mAb conferred a significant survival advantage compared with PBS pretreatment ($p = 0.045$ by log-rank test; Fig. 1D), suggesting that preservation of the alveolar–endothelial barrier during the insult improves outcomes after returning to normoxia.

In BAL fluid, EphA2 mAb treatment decreased levels of IL-10 and TNF-α and tended to reduce IL-6, although not all changes reached statistical significance (Fig. 1E). Because the lungs were harvested immediately after prolonged hyperoxia, secondary inflammatory cascades may have been incompletely developed at the time of sampling, potentially blunting detectable differences.

EphA2 blockade preserves junctional proteins and modulates Akt/Bcl-2 signaling

Western blot analysis demonstrated that EphA2 mAb pretreatment effectively suppressed the hyperoxia-induced phosphorylation of EphA2 and reduced ephrinA1 expression (Fig. 2; Additional File. 4). Importantly, the EphA2 mAb restored the expression of key junctional proteins that were disrupted by hyperoxia. VE-cadherin, E-cadherin, and ZO-2 levels, which decreased in hyperoxic PBS-treated lungs, were markedly preserved in the EphA2 mAb group (Fig. 2).

Simultaneously, the EphA2 blockade influenced intracellular survival pathways. Phosphorylated Akt further increased in EphA2 mAb-treated lungs compared with the hyperoxic control lungs, whereas Bcl-2 expression was reduced (Fig. 2). Although the precise mechanisms underlying these changes remain to be clarified, these

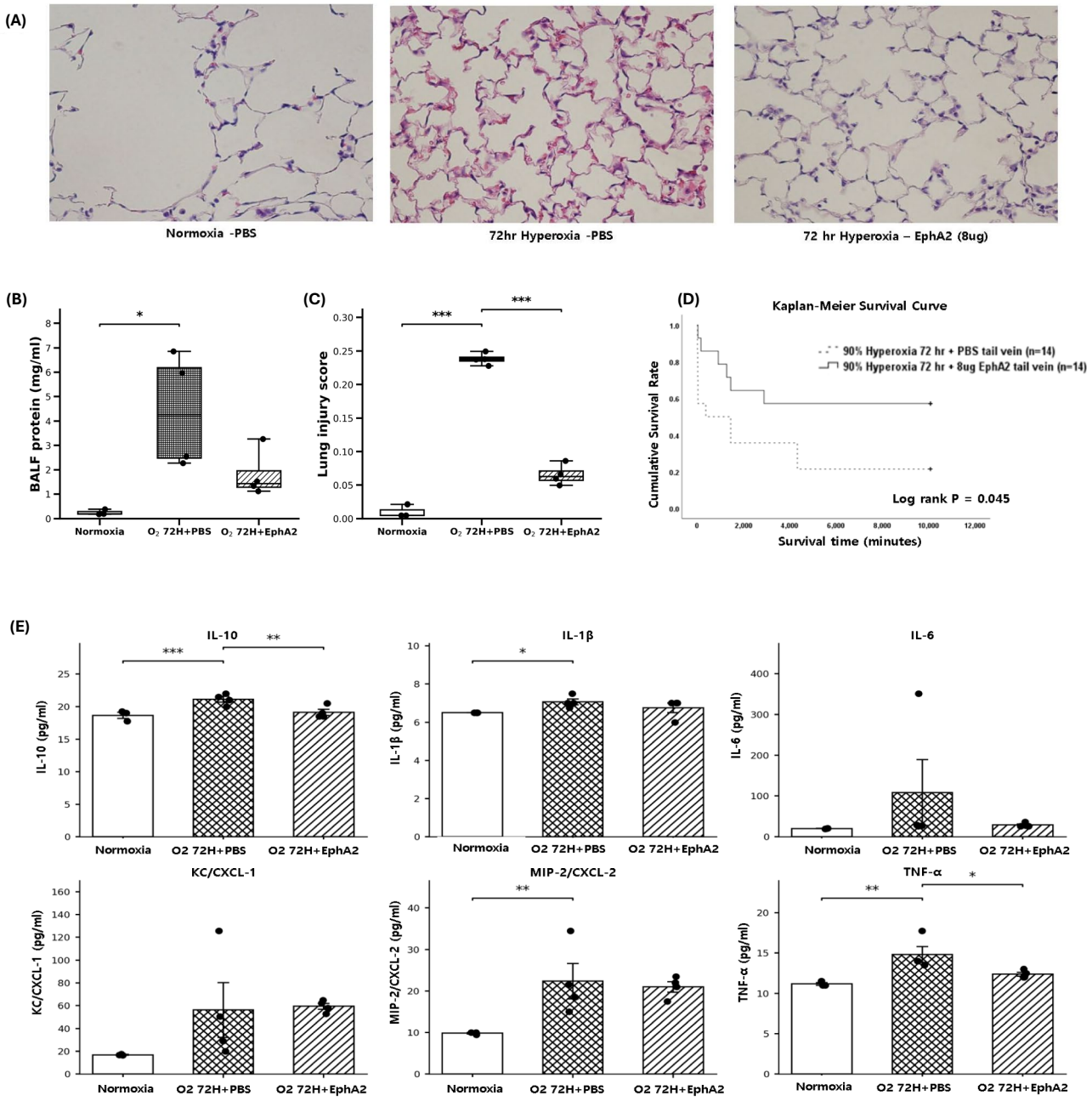

Fig. 1. EphA2 monoclonal antibody (mAb) protects against hyperoxia-induced acute lung injury (HALI) in model mice. (**A**) Hematoxylin and eosin (H&E)-stained lung sections show reduced vascular engorgement, hyaline membrane formation, and alveolar edema in the EphA2 mAb group. (**B**) BAL fluid protein concentrations showed a decreasing trend in the EphA2 mAb group compared with the PBS group under hyperoxia. In (**B**), the asterisk (*) indicates the comparison between Normoxia and O_2 72H + PBS. (**C**) Lung injury scores were lower in the EphA2 mAb group compared with the PBS group. (**D**) EphA2 mAb improved survival after 72 h hyperoxia compared with PBS (log-rank p = 0.045; n = 14 per group). (**E**) Cytokine analysis of BAL fluid shows lower IL-10 and TNF-α in the EphA2 mAb group. In (**E**), statistical comparisons were performed using unpaired two-tailed t-tests for the indicated pairwise comparisons (Normoxia vs O_2 72H + PBS and O_2 72H + PBS vs O_2 72H + EphA2). In (**B**) and (**C**), data are presented as median (IQR). In (**E**), data are presented as mean ± SEM. Each dot represents one mouse (biological replicate; normoxia n = 3, O_2 72H + PBS n = 4, O_2 72H + EphA2 n = 4). *p < 0.05, **p < 0.01, ***p < 0.001 (where indicated).

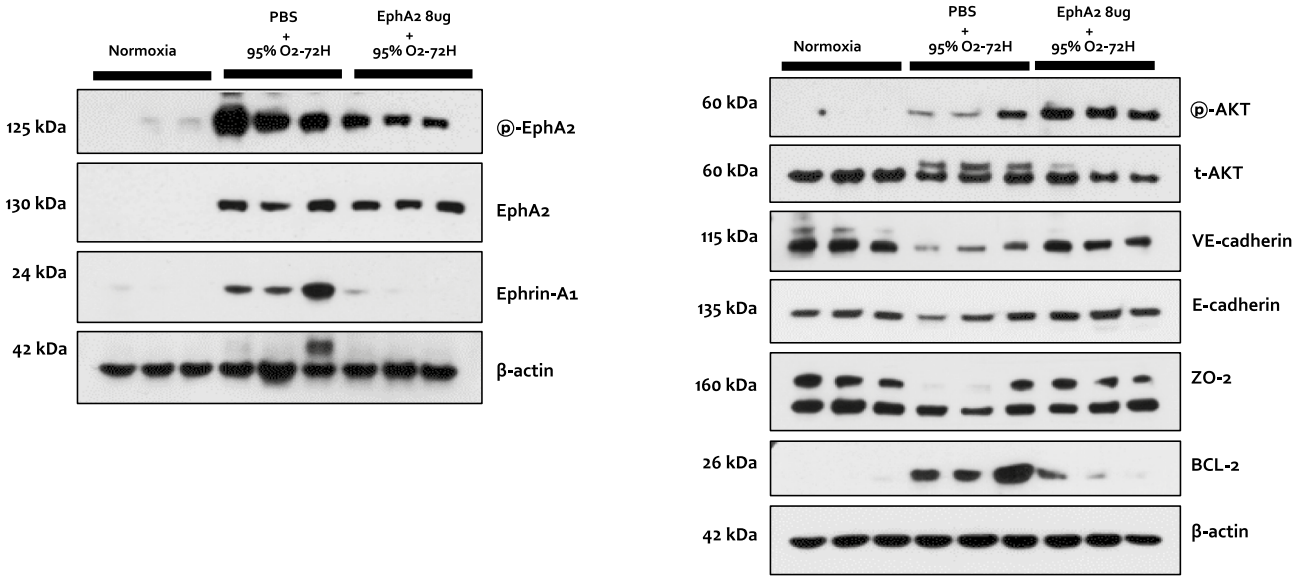

Fig. 2. Western blot analysis of the effect of the EphA2 monoclonal antibody (mAb) on the hyperoxia-induced acute lung injury (HALI) mouse model. (**A**) Western blot analysis showed that phosphorylated EphA2 and EphrinA1 were suppressed by EphA2 mAb. Treatment with EphA2 mAb restored the expression of VE-cadherin and E-cadherin. The EphA2 mAb further activated phosphorylated Akt and decreased Bcl-2 expression. (*$p < 0.05$, **$p < 0.01$, ***$p < 0.001$). For presentation, bands were cropped from the same original membranes, and any non-adjacent lanes are separated by white spaces. Uncropped images of the corresponding membrane pieces with boundaries and edges visible are provided in Supplementary Fig S1.

observations suggest that EphA2 inhibition may shift the balance of signaling to stabilize endothelial–epithelial junctions while modulating apoptotic responses.

EphA2 monoclonal antibody maintains VEGF and claudin-5 expression and VE-cadherin localization

Immunohistochemical staining corroborated the western blot results. In hyperoxic PBS-treated mice, VEGF and claudin-5 expression in the pulmonary vasculature and alveolar walls were diminished, and VE-cadherin staining along the endothelial borders, particularly in the peripheral lungs, was markedly disrupted. EphA2 mAb treatment preserved VEGF and claudin-5 staining and restored continuous VE-cadherin localization at cell–cell junctions (Fig. 3A–C). These data support the conclusion that EphA2 blockade helps maintain the structural integrity of the alveolar–endothelial barrier during hyperoxic stress.

EphA2 blockade reduces oxidative stress in hyperoxic lungs

To assess oxidative stress, we performed IF staining for 4-HNE, a lipid peroxidation product, and E-cadherin to identify alveolar epithelial cells. In hyperoxic PBS-treated lungs, the 4-HNE signal markedly increased in epithelial cells, consistent with substantial oxidative injury. In contrast, the EphA2 mAb reduced 4-HNE staining in E-cadherin-positive cells (Fig. 4), indicating that EphA2 blockade mitigates hyperoxia-induced oxidative damage in the alveolar epithelium.

Discussion

In this experimental study, we demonstrated that EphA2/ephrinA1 signaling was activated in a murine model of HALI and that pharmacological EphA2 blockade through monoclonal antibody administration attenuated lung injury, preserved the alveolar–endothelial barrier, and improved survival following a severe hyperoxic insult. Our data added to the prior work on the role of EphA2/ephrinA1 in lung injury and supported EphA2 blockade as a potential barrier-protective strategy under severe hyperoxic exposure.

Consistent with previous reports, prolonged exposure to high-inspired oxygen fractions led to progressive disruption of the alveolar–capillary barrier, increased BAL protein leakage, and caused a robust inflammatory response characterized by elevated IL-1β, IL-6, TNF-α, and MIP-2. The histological features typical of HALI, including alveolar edema, hyaline membranes, and interstitial inflammation, became more pronounced with prolonged exposure to hyperoxia. In parallel, the expression of tight and adherens junction proteins, such as VE-cadherin, claudin-5, VEGF, and ZO-2, decreased, highlighting the structural disintegration of both endothelial and epithelial barriers.

We observed a clear temporal association between hyperoxia and the activation of EphA2/ephrinA1 signaling in the lungs, whereas EphB4/ephrinB2 changes were less prominent. This pattern is consistent with previous studies showing that EphA2 is upregulated in experimental lung injury models, including bleomycin- and VILI models, and that EphA2 activation promotes endothelial permeability and inflammatory cell recruitment[21–23].

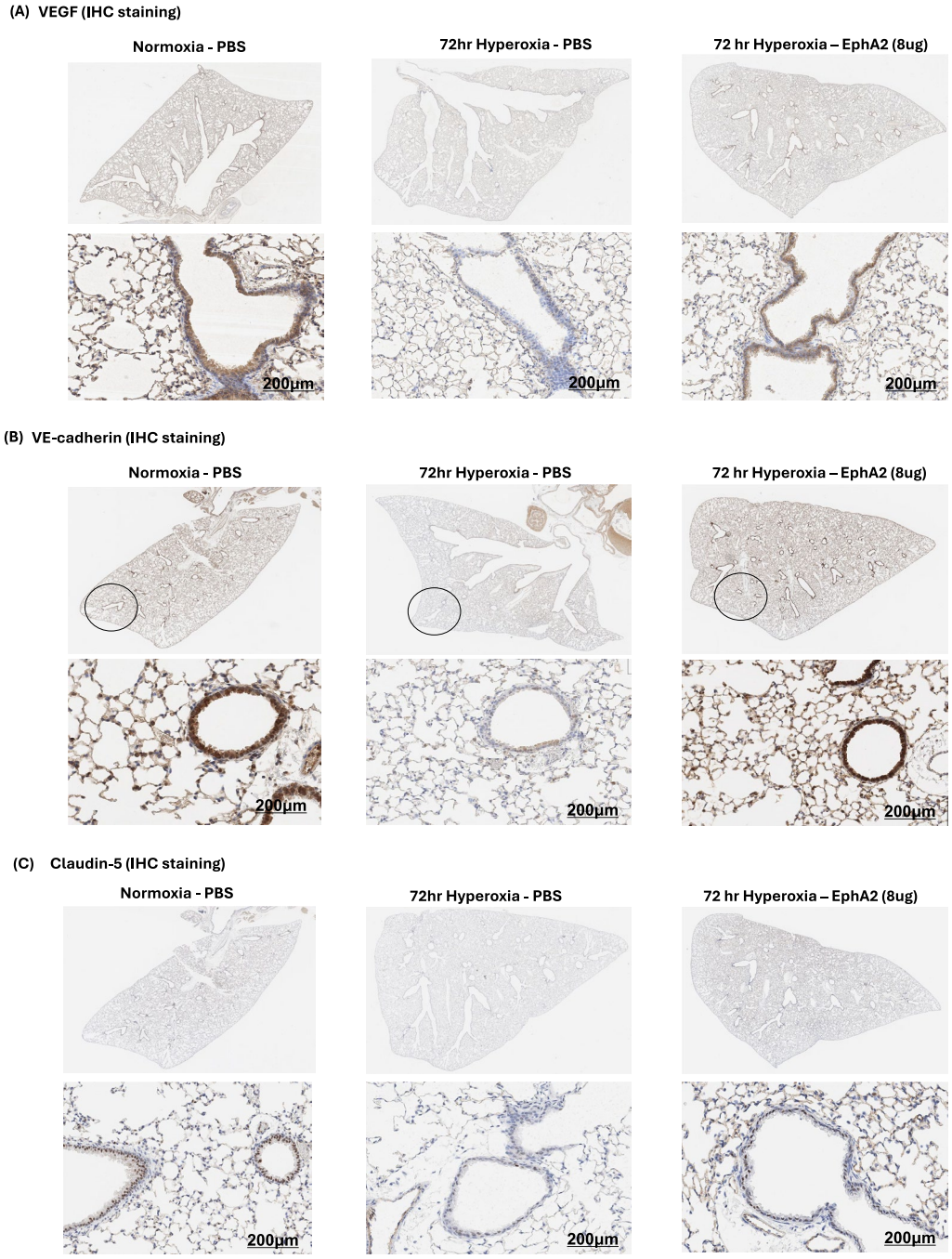

Fig. 3. Immunohistochemical staining for the effect of EphA2 monoclonal antibody (mAb) on the hyperoxia-induced acute lung injury (HALI) mouse model. The EphA2 mAb restored VEGF (**A**) and claudin-5 expression as shown by immunohistochemical (IHC) staining (**C**). EphA2 mAb restored VE-cadherin expression (**B**) at the edges of mouse lungs, as shown by IHC staining. (*$p < 0.05$, **$p < 0.01$, ***$p < 0.001$).

Taken together, these data support a model in which hyperoxia triggers EphA2/ephrinA1 signaling, which in turn contributes to cytoskeletal remodeling, junctional disruption, and increased vascular leak.

Blocking EphA2 with an mAb exerts multiple protective effects. Histologically, EphA2 mAb reduced edema, hyaline membranes, and inflammatory infiltration, resulting in significantly lower lung injury scores. At the functional level, BAL protein concentrations showed a downward trend, and post-hyperoxic survival significantly improved. The survival benefit was particularly notable because the insult was severe (72 h of > 95% oxygen), and even the modest preservation of barrier function during this period likely had a large impact once the animals were returned to room air.

Mechanistically, the EphA2 blockade stabilizes the key junctional proteins critical for barrier integrity. VE-cadherin and claudin-5 are essential components of the adherens and tight junctions in the pulmonary

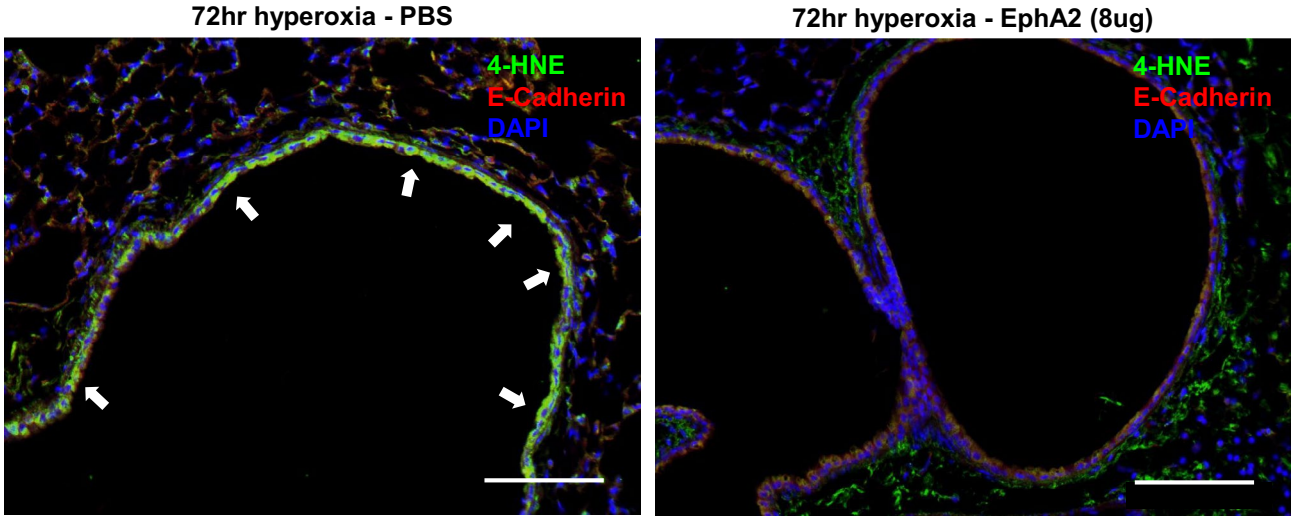

Fig. 4. Effect of EphA2 monoclonal antibody (mAb) on oxidative stress of hyperoxia-induced acute lung injury (HALI). The EphA2 mAb suppresses oxidative stress in lungs during hyperoxia-induced acute lung injury. Representative immunostaining of 4-HNE (green) in lung epithelial cells (E-Cadherin, Red) during hyperoxia-induced acute lung injury. (4-HNE is an oxidative stress marker).

endothelium, and their degradation is a hallmark of increased vascular permeability. In our study, EphA2 mAb preserved VE-cadherin, E-cadherin, claudin-5, ZO-2, and VEGF expression and maintained VE-cadherin localization at endothelial borders, suggesting that interrupting the EphA2 signaling prevents junctional disassembly during hyperoxic stress. These findings are consistent with those of previous in vitro studies showing that ephrinA1/EphA2 activation induces rearrangement and internalization of junctional proteins, leading to increased permeability[14,15,23–26].

The observed changes in Akt and Bcl-2 further support the role of EphA2 in modulating cell survival pathways in HALI. Hyperoxia alone induces transient Akt phosphorylation and Bcl-2 upregulation, reflecting the activation of pro-survival signaling in response to oxidative injury. Interestingly, treatment with EphA2 mAb was associated with increased Akt phosphorylation and reduced Bcl-2 expression[27,28]. One possible interpretation is that EphA2 blockade alters upstream signaling such that Akt-mediated barrier-stabilizing effects are maintained, whereas anti-apoptotic signaling normalizes as the overall injury burden decreases[29]. However, our data do not allow definitive mechanistic conclusions and additional studies using genetic models are needed to dissect these pathways.

EphA2 mAb also reduced oxidative stress, as evidenced by decreased 4-HNE accumulation in alveolar epithelial cells[30,31]. HALI is partially driven by excess ROS generation, which overwhelms endogenous antioxidant defenses and damages lipids, proteins, and DNA[32,33]. By limiting oxidative injury in epithelial cells, EphA2 blockade may interrupt feed-forward cycles of inflammation and barrier disruption, further contributing to lung protection[18].

With respect to clinical relevance, we emphasize that HALI does not recapitulate the full complexity of ARDS and VILI, in which mechanical stress and regional heterogeneity are major drivers of injury. Instead, our findings are most directly applicable to clinical scenarios in which high FiO_2 exposure is sustained and may become a dominant contributor to barrier disruption —for example, neurologic patients receiving hyperoxic support, post-cardiac arrest management, or conditions such as aeromedical evacuation where oxygen delivery constraints lead to prolonged high inspired oxygen fractions.

Our study has several limitations. First, we used a pharmacological approach and did not use EphA2- or ephrinA1-deficient mice. Although the specificity of the EphA2 mAb and the consistency of our findings support a causal role for EphA2, genetic models would provide more definitive evidence. Second, we did not directly address why alveolar endothelial cells appear particularly vulnerable in HALI, nor did we separately quantify the endothelial versus epithelial contributions to barrier failure. High-resolution imaging and cell type–specific approaches are required to elucidate how EphA2 signaling operates in distinct pulmonary compartments. Third, we focused on pretreatment with a single dose of EphA2 mAb, reflecting the technical constraints of repeated injections into a sealed hyperoxia chamber. Clinically, prolonged high FiO_2 exposure is often anticipated in selected settings (e.g., neurologic indications or situations where lower oxygen targets cannot be safely maintained); therefore, prophylactic targeting may be feasible in such contexts. Future studies should evaluate therapeutic windows and dosing regimens that better reflect clinical practice. Lastly, we only used male C57BL/6 J mice; therefore, sex as a biological variable may influence HALI susceptibility and EphA2-related signaling. Future studies should include both sexes and evaluate sex-stratified effects.

Despite these limitations, this study has several important implications. From a mechanistic standpoint, it strengthens the concept that EphA2/ephrinA1 signaling is a central regulator of alveolar–endothelial barrier integrity under injurious conditions, extending this role from endotoxin- and ventilator-induced injury to hyperoxia. From a translational perspective, these data suggest that EphA2-directed approaches may mitigate

oxygen-induced lung damage, particularly in clinical scenarios in which lower oxygen targets cannot be safely maintained. Finally, because oxygen therapy is ubiquitous in critical care, strategies that blunt its toxic effects without compromising the gas exchange could have a broad impact.

Conclusion

In a murine model of HALI, EphA2/ephrinA1 signaling was activated in parallel with the disruption of junctional proteins, oxidative stress, and inflammation. Pharmacological blockade of EphA2 with a monoclonal antibody preserved alveolar–endothelial junctional integrity, reduced histological injury and protein leakage, attenuated inflammatory and oxidative responses, and improved survival after severe hyperoxic insult. These findings support a proof-of-concept that EphA2 blockade can preserve barrier integrity under severe hyperoxic stress, warranting further studies to define therapeutic windows and dosing regimens.

Data availability

All data generated or analysed during this study are included in this published article and its supplementary files.

Received: 4 December 2025; Accepted: 18 March 2026
Published online: 25 March 2026

References

1. Singer, M. et al. Dangers of hyperoxia. *Crit. Care* **25**, 440. https://doi.org/10.1186/s13054-021-03815-y (2021).
2. Lius, E. E. & Syafaah, I. Hyperoxia in the management of respiratory failure: A literature review. *Ann. Med. Surg. (Lond.)* **81**, 104393. https://doi.org/10.1016/j.amsu.2022.104393 (2022).
3. Su, Y., Lucas, R., Fulton, D. J. R. & Verin, A. D. Mechanisms of pulmonary endothelial barrier dysfunction in acute lung injury and acute respiratory distress syndrome. *Chin. Med. J. Pulmonary Crit. Care Med.* **2**, 80–87. https://doi.org/10.1016/j.pccm.2024.04.002 (2024).
4. Wang, F. et al. Oxidative stress in ARDS: Mechanisms and therapeutic potential. *Front. Pharmacol.* **16**, 1603287. https://doi.org/10.3389/fphar.2025.1603287 (2025).
5. Schjørring, O. L. et al. Lower or higher oxygenation targets for acute hypoxemic respiratory failure. *N. Engl. J. Med.* **384**, 1301–1311. https://doi.org/10.1056/NEJMoa2032510 (2021).
6. Li, X. et al. Conservative versus liberal oxygen therapy for intensive care unit patients: Meta-analysis of randomized controlled trials. *Ann. Intensive Care* **14**, 68. https://doi.org/10.1186/s13613-024-01300-7 (2024).
7. Wang, J. et al. Conservative versus liberal oxygen therapy for critically ill patients: A meta-analysis with trial sequential analysis and clinical recommendations. *J. Transl. Crit. Care Med.* **7**, e25. https://doi.org/10.1097/JTCCM-D-25-00005 (2025).
8. Young, P. J. Less is best for oxygen therapy in adults in the intensive care unit with severe hypoxaemia due to COVID-19. *Intensive Care Med.* **50**, 1685–1687. https://doi.org/10.1007/s00134-024-07554-w (2024).
9. Lilien, T. A., van Meenen, D. M. P., Schultz, M. J., Bos, L. D. J. & Bem, R. A. Hyperoxia-induced lung injury in acute respiratory distress syndrome: What is its relative impact?. *Am. J. Physiol. Lung Cell. Mol. Physiol.* **325**, L9–L16. https://doi.org/10.1152/ajplung.00443.2022 (2023).
10. Zhou, X., Tian, L., Xiong, W., Li, Y. & Liu, Q. Ferroptosis and hyperoxic lung injury: Insights into pathophysiology and treatment approaches. *Front. Pharmacol.* **16**, 1568246. https://doi.org/10.3389/fphar.2025.1568246 (2025).
11. Tiboldi, A. et al. Effects of hyperoxia and hyperoxic oscillations on the proteome of murine lung microvascular endothelium. *Antioxidants* **11**, 2349. https://doi.org/10.3390/antiox11122349 (2022).
12. Ren, Y. et al. Hyperoxia can induce lung injury by upregulating AECII autophagy and apoptosis via the mTOR pathway. *Mol. Biotechnol.* **66**, 3357–3368. https://doi.org/10.1007/s12033-023-00945-2 (2024).
13. Psilopatis, I. et al. EPH/Ephrin targeting revolutionize lung cancer treatment?. *Int. J. Mol. Sci.* **24**, 93. https://doi.org/10.3390/ijms24010093 (2023).
14. Chen, Y. et al. EphrinA1/EphA2 promotes epithelial hyperpermeability involving lipopolysaccharide-induced intestinal barrier dysfunction. *J. Neurogastroenterol. Motil.* **26**, 397–409. https://doi.org/10.5056/jnm19095 (2020).
15. Carpenter, T. C., Schroeder, W., Stenmark, K. R. & Schmidt, E. P. EphA2 promotes permeability and inflammatory responses to bleomycin-induced lung injury. *Am. J. Respir. Cell Mol. Biol.* **46**, 40–47. https://doi.org/10.1165/rcmb.2011-0044OC (2012).
16. Good, R. J. et al. MicroRNA dysregulation in lung injury: The role of the miR-26a/EphA2 axis in regulation of endothelial permeability. *Am. J. Physiol. Lung Cell. Mol. Physiol.* **315**, L584–L594. https://doi.org/10.1152/ajplung.00073.2017 (2018).
17. Hong, J. Y. et al. EphA2 receptor signaling mediates inflammatory responses in lipopolysaccharide-induced lung injury. *Tuberc. Respir. Dis.* **78**, 218–226. https://doi.org/10.4046/trd.2015.78.3.218 (2015).
18. Feng, G. et al. EphA2 antagonism alleviates LPS-induced acute lung injury via Nrf2/HO-1, TLR4/MyD88 and RhoA/ROCK pathways. *Int. Immunopharmacol.* **72**, 176–185. https://doi.org/10.1016/j.intimp.2019.04.008 (2019).
19. Shin, J. M. et al. EphA1 and EphA2 signaling modulates epithelial permeability in human sinonasal epithelial cells, and rhinovirus infection induces epithelial barrier dysfunction via EphA2 receptor signaling. *Int. J. Mol. Sci.* **24**, 3629. https://doi.org/10.3390/ijms24043629 (2023).
20. Fukuda, R., Beppu, S., Hinata, D., Kamada, Y. & Okiyoneda, T. Perturbation of EPHA2 and EFNA1 trans binding amplifies inflammatory response in airway epithelial cells. *iScience* **28**, 111872. https://doi.org/10.1016/j.isci.2025.111872 (2025).
21. Lee, S. H. et al. NADPH oxidase 4 signaling in a ventilator-induced lung injury mouse model. *Respir. Res.* **23**, 73. https://doi.org/10.1186/s12931-022-01992-0 (2022).
22. Park, B. H. et al. Erythropoietin-producing hepatoma receptor tyrosine kinase A2 modulation associates with protective effect of prone position in ventilator-induced lung injury. *Am. J. Respir. Cell Mol. Biol.* **58**, 519–529. https://doi.org/10.1165/rcmb.2017-0143OC (2018).
23. Ojima, T. et al. EphrinA1 inhibits vascular endothelial growth factor-induced intracellular signaling and suppresses retinal neovascularization and blood-retinal barrier breakdown. *Am. J. Pathol.* **168**, 331–339. https://doi.org/10.2353/ajpath.2006.050435 (2006).
24. Larson, J., Schomberg, S., Schroeder, W. & Carpenter, T. C. Endothelial EphA receptor stimulation increases lung vascular permeability. *Am. J. Physiol. Lung Cell. Mol. Physiol.* **295**, L431–L439. https://doi.org/10.1152/ajplung.90256.2008 (2008).
25. Cercone, M. A., Schroeder, W., Schomberg, S. & Carpenter, T. C. EphA2 receptor mediates increased vascular permeability in lung injury due to viral infection and hypoxia. *Am. J. Physiol. Lung Cell. Mol. Physiol.* **297**, L856–L863. https://doi.org/10.1152/ajplung.00118.2009 (2009).
26. Darling, T. K. et al. EphA2 contributes to disruption of the blood–brain barrier in cerebral malaria. *PLoS Pathog.* **16**, e1008261. https://doi.org/10.1371/journal.ppat.1008261 (2020).

27. O'Reilly, M. A. et al. Bcl-2 family gene expression during severe hyperoxia-induced lung injury. *Lab. Invest.* **80**, 1845–1854. https://doi.org/10.1038/labinvest.3780195 (2000).
28. Truong, S. V. et al. Extracellular signal-regulated kinase activation delays hyperoxia-induced epithelial cell death under conditions of Akt downregulation. *Am. J. Respir. Cell Mol. Biol.* **31**, 611–618. https://doi.org/10.1165/rcmb.2004-0141OC (2004).
29. Miao, H. et al. EphA2 mediates ligand-dependent inhibition and ligand-independent promotion of cell migration and invasion via a reciprocal regulatory loop with Akt. *Cancer Cell* **16**, 9–20. https://doi.org/10.1016/j.ccr.2009.04.009 (2009).
30. Sidramagowda Patil, S. et al. Alda-1 attenuates hyperoxia-induced acute lung injury in mice. *Front. Pharmacol.* **11**, 597942. https://doi.org/10.3389/fphar.2020.597942 (2021).
31. Galam, L., Failla, A., Soundararajan, R., Lockey, R. F. & Kolliputi, N. 4-Hydroxynonenal regulates mitochondrial function in human small airway epithelial cells. *Oncotarget* **6**, 41508–41521. https://doi.org/10.18632/oncotarget.6131 (2015).
32. Dean, J. B., Mulkey, D. K., Henderson, R. A., Potter, S. J. & Putnam, R. W. Hyperoxia, reactive oxygen species, and hyperventilation: Oxygen sensitivity of brain stem neurons. *J. Appl. Physiol.* **96**, 784–791. https://doi.org/10.1152/japplphysiol.00892.2003 (2004).
33. Carnesecchi, S. M. et al. NADPH oxidase-1 plays a crucial role in hyperoxia-induced acute lung injury in mice. *Am. J. Respir. Crit. Care Med.* **180**, 972–981. https://doi.org/10.1164/rccm.200902-0296OC (2009).

Author contributions
KSC designed the hypotheses and experiments and wrote the first draft of the manuscript. KSC and JHS conducted experiments. SHL, AYL, and MSP provided feedback. JSM and YSK guided the study and revised the manuscript.

Funding
This research was supported by the Basic Science Research Program through the National Research Foundation of Korea (NRF), funded by the Ministry of Science, ICT, and Future Planning (NRF-2014R1A1A1038278).

Declarations

Competing interests
The authors declare no competing interests.

Ethics approval and consent to participate
All animal procedures were reviewed and approved by the Institutional Animal Care and Use Committee (IACUC-2013-0307) of the Yonsei University College of Medicine (Seoul, South Korea) and were conducted in accordance with the National Institutes of Health Guidelines for the Care and Use of Laboratory Animals. Male wild-type C57BL/6 J mice (8–10 weeks old, 20–24 g; Orient Bio, Seongnam, South Korea) were housed under controlled temperature and a 12 h–12 h light–dark cycle with free access to standard chow and water. All mice were specific pathogen-free and acclimatized for at least 7 days before experimentation. No prespecified exclusion criteria were applied, and no animals were excluded from the analyses. Mice were euthanized by intraperitoneal injection of a lethal dose (2–3 times the standard anesthetic dose) of Zoletil (30 mg/kg) and xylazine (Rompun, 10 mg/kg), after which bronchoalveolar lavage fluid and lung tissue were collected. The study is reported in accordance with the ARRIVE 2.0 guidelines.

Additional information
Supplementary Information The online version contains supplementary material available at https://doi.org/10.1038/s41598-026-45319-1.

Correspondence and requests for materials should be addressed to J.S.M. or Y.S.K.